EFFECTIVE ANTENNA TEMPERATURE FROM TERRESTRIAL AND COSMIC NOISE IN THE 0.1- TO 40.0-Gc BAND

A. NAPARSTEK

Navigation and Guidance Laboratory, Avionics, ASRWG
AERONAUTICAL SYSTEMS DIVISION
AIR FORCE SYSTEMS COMMAND
Wright-Patterson Air Force Base, Ohio

Prepared under Contract No. AF 33(616)-8244 by

COUNTERMEASURES DEPARTMENT
Institute of Science and Technology
THE UNIVERSITY OF MICHIGAN

March 1963

4515-20-T

EFFECTIVE ANTENNA TEMPERATURE FROM TERRESTRIAL AND COSMIC NOISE IN THE 0.1- TO 40.0-Gc BAND

A. NAPARSTEK

Navigation and Guidance Laboratory, Avionics, ASRWG
AERONAUTICAL SYSTEMS DIVISION
AIR FORCE SYSTEMS COMMAND
Wright-Patterson Air Force Base, Ohio

Project No. 1 (620-5191)
Task No. 50927

March 1963

Contract No. AF 33(616)-8244

Countermeasures Department
Institute of Science and Technology
THE UNIVERSITY OF MICHIGAN
Ann Arbor, Michigan

NOTICES

Sponsorship. The work reported herein was conducted by the Institute of Science and Technology for the U. S. Air Force, Contract AF 33(616)-8244. Contracts and grants to The University of Michigan for the support of sponsored research by the Institute of Science and Technology are administered through the Office of the Vice-President for Research.

ASTIA Availability. Qualified requesters may obtain copies of this document from:

Armed Services Technical Information Agency
Arlington Hall Station
Arlington 12, Virginia

Final Disposition. After this document has served its purpose, it may be destroyed. Please do not return it to the Institute of Science and Technology.

FOREWORD

This is a technical report prepared by the Institute of Science and Technology at The University of Michigan, Ann Arbor, on Air Force contract AF 33(616)-8244 under Task No. 50927 of Project No. 1(620-5191). The work was administered under the direction of Navigation and Guidance Laboratory, Avionics, ASRWG, Aeronautical Systems Division. Evan Larkin was project engineer for the laboratory.

CONTENTS

FIGURES

TABLES

EFFECTIVE ANTENNA TEMPERATURE FROM TERRESTRIAL AND COSMIC NOISE IN THE 0.1- TO 40.0-Gc BAND

ABSTRACT

This report presents a derivation of an expression for the effective antenna temperature for an antenna viewing a multitude of discrete and distributed radio-frequency noise sources. The presentation makes use of concepts, parameters, and units that have been introduced in radio astronomy for the purpose of describing measurements of radio-frequency radiation of extraterrestrial origin.

The report also presents a comprehensive review and analysis of current knowledge of and available data on radio-frequency noise of terrestrial and extraterrestrial origin in the 0.1- to 40.0-Gc frequency band. These data, together with the derived equation for the effective antenna temperature, will enable one to calculate the effective antenna temperature for any antenna located on the earth's surface, provided the normalized power pattern, the directivity, and the efficiency of the antenna are known. The report also shows how to determine realistic bounds for the effective antenna temperature of antennas located in aerospace.

Analysis of the data on the various noise sources shows that, even for some presently available receiving systems (which use masers as preamplifiers), the external noise will exceed the internally generated noise (referred to the receiver input terminals) of the receiver for certain orientations of the antenna. From the standpoint of external noise considerations only, the optimum frequency band lies between 2 and 8 Gc.

1
INTRODUCTION

The practicality of extremely-low-internal-noise microwave receivers employing masers and parametric amplifiers has been successfully demonstrated in radio astronomy (microwave radiometers), radar observations of Venus, and ultra-low-noise measurements [1, 2, 3, 4]. The noise that appears at the output terminals of a receiving antenna is an important possible limiting factor on overall noise performance of such a receiving system. To exploit fully the low-internal-noise temperatures of these devices, which will be used in future space communication and radar systems, one must make a careful quantitative examination of the sources of external noise to see how that noise may best be minimized by frequency selection, by spatial discrimina-

This report was released by the author in December 1962 for publication as an ASD Technical Note.

tion to avoid intense noise sources in particular applications, and by optimizing the design of the antenna with respect to the beamwidth, side lobes, and receiver-input waveguide.

It is assumed that a receiving system operating in the frequency range of 0.1 Gc to 40 Gc is located at some point P in aerospace or on the surface of the earth. The purpose of the investigation was to describe, quantitatively and qualitatively, the external noise that appears at the antenna output terminals of this receiving system and to determine what proportion of this noise is contributed by each of the various sources as a function of the receiving system's operating frequency.

This report presents a derivation of an expression for the effective antenna temperature, valid for the most general situation of an antenna viewing a multitude of discrete and distributed radio-frequency noise sources. Concepts, parameters, and units that have been introduced in radio astronomy are used in the presentation.

The report also presents a comprehensive review and analysis of current knowledge of and available data on radio-frequency noise of terrestrial and extraterrestrial origin in the 0.1- to 40.0-Gc frequency band. These data, together with the derived equation for the effective antenna temperature, will enable one to calculate the effective antenna temperature for any antenna located on the earth's surface, provided that the normalized power pattern, the directivity, and the efficiency of the antenna are known. In addition, this report describes a method for determining realistic bounds on the effective antenna temperature for antennas in aerospace.

Analysis of the data on the various noise sources shows that, even for some currently available receiving systems (which use masers as preamplifiers), the external noise will exceed the internally generated noise (referred to the receiver input terminals) of the receiver for certain orientations of the antenna. From the standpoint of external noise considerations only, the optimum frequency band lies between 2 and 8 Gc.

2
DEFINITION OF EFFECTIVE ANTENNA TEMPERATURE

It has become standard practice to describe the noise that appears at the output terminals of a receiving antenna in terms of a temperature known as the "effective antenna temperature." The effective antenna temperature, at a frequency f within a frequency band β centered about f, is defined as that temperature at which the available output power, due to thermal agitation, from a lossy linear network is equal to the available noise power at the antenna output terminals in the frequency band β.

For a lossy linear network at temperature T, the available output noise power in the frequency band β centered about any frequency f is given by

$$P_N = kT\beta$$

where P_N is the available output noise power in watts

k is Boltzmann's constant (1.3803×10^{-23} joule/^oK)

T is the temperature of the network in ^oK

β is the frequency band in cps

Therefore, according to the above definition of effective antenna temperature, the formula

$$P_N = kT_a\beta \tag{1}$$

gives the numerical relation between the available noise power P_N at the antenna and the effective antenna temperature T_a.

It should be noted that T_a does not depend on the impedance of the load that is connected to the antenna under actual operating conditions. This means that when a receiver is connected to the antenna through a transmission line, the actual measured noise power may not equal the available noise power at the antenna output terminals because the combination of transmission line and receiver may not comprise a matched load for the antenna. However, since for the purpose of determining the sensitivity of a receiving system one is concerned only with the ratio of signal power to noise power, and since this ratio of powers at the antenna output terminals remains the same whether the load is matched or unmatched, the above definition of effective antenna temperature is a sensible one.

Since the available output noise power at the antenna will generally be a function of both frequency and antenna orientation, it follows that the effective antenna temperature will also be a function of both frequency and antenna orientation.

The concept of an effective antenna temperature is physically very meaningful because, as the ensuing analysis will show, it is very simply related to certain temperatures which are used in specifying the radio noise incident on the antenna from the various noise sources.

3

CONCEPTS, PARAMETERS, AND UNITS USED TO DESCRIBE RADIO-FREQUENCY NOISE

In radio astronomy, there are two systems of units to describe the strength of incoherent electromagnetic radiation (radio noise): an electromagnetic system and a temperature system.

In this report, the temperature system will be used because of its simplicity and because it allows one to relate the effective antenna temperature to certain temperatures which will be associated with the radio noise incident at the antenna.

In the electromagnetic system, the quantitative description of the strength of noise radiation at a given frequency from a given direction in space at an observation point P is in terms of two quantities, b (brightness) and S (flux density). The use of either quantity depends upon the source "associated" with the radiation. The term "flux density" usually applies to a source of very small angular size (as seen from the observation point P) and the term "brightness" to an extended source, such as a part of the sky. More precisely, noise sources are usually classified as discrete or distributed. The distributed sources are those that produce a fairly smooth spatial variation of noise over a solid angle (as seen at the observation point P) which is larger than the solid angle subtended on the earth by the solar disk (mean solid angle subtended by the photosphere is 6.8×10^{-5} sterad). The discrete sources are those that emit in a given direction very intense radiation relative to the continuous background radiation in neighboring directions over a solid angle which is less than or equal to that subtended by the solar disk. In this definition, reference is not made to any physical objects associated with the sources, but merely to certain solid angular extents from which radiation is arriving, because, in studies of extraterrestrial radiation, it has not yet been possible to associate any specific physical objects with many of the sources. Further, the distinction between discrete and distributed cosmic sources depends on the sensitivity and resolution of currently available radio telescopes [5, pp. 24-25, 231-278].

At a point P, the flux density from a discrete source is defined by

$$S = \frac{\Delta E}{(\Delta A)(\Delta f)(\Delta t)} \tag{2}$$

where S is the flux density at P (w/meter^2-cps)

f is the frequency under consideration (cps)

Δf is a small frequency band centered about f (cps)($\Delta f \ll f$)

ΔA is an incremental area in the wavefront at P (meter^2)

Δt is a time interval (sec)($\Delta t \gg \frac{1}{f}$)

ΔE is the energy flowing through ΔA in the band Δf (joules)

If the source of radiation is a distributed source, one considers an incremental solid angle cone of $\Delta\Omega$ steradians which has its vertex at P and which is centered about the direction being observed. If the flux density within $\Delta\Omega$ is ΔS, then the brightness b is defined by

$$b = \lim_{\Delta\Omega \to 0} \frac{\Delta S}{\Delta\Omega} \text{ w/meter}^2\text{-cps-sterad} \tag{3}$$

If one assumes that the noise radiation incident at P is stationary with time, then S will be a function of frequency only and b will be a function of frequency and direction only. The assumption of stationarity of the noise radiation over a sufficiently small time interval is, as will be shown later, quite reasonable for most of the noise sources which contribute significantly to the effective antenna temperature.

Flux density is appropriate for specifying the noise radiation from the sun, the moon, the planets, and the discrete cosmic sources variously called "radio stars" or "radio galaxies," and is used in describing measurements of noise radiation by antennas whose beamwidths are large compared to the angular size of the source. Brightness is used to specify the distribution of the strength of the cosmic background radiation over the celestial sphere, and the strength of other extended sources such as the atmosphere. The polarization of the noise radiation must be considered when the values of b and S are being specified. If the polarization is random, as it is with most noise radiation, then an antenna will accept only one polarized component of the wave (i.e., only half the incident power regardless of the particular polarization accepted by the antenna). The quantities S and b are, however, twice the value of any one linearly, circularly, or elliptically polarized component.

The definition of the available noise power at the output terminals of the antenna in terms of a temperature—the effective antenna temperature—would not be meaningful in the physical sense unless it were related in some way to the actual kinetic temperatures of thermally radiating bodies. The transformation of the electromagnetic quantities b and S to corresponding temperatures of thermal radiators is obtained by using Planck's law of radiation, involving the extremely useful concept of blackbody radiation. This law is given by the formula

$$B_f = \frac{2hf^3}{c^2} \cdot \frac{1}{\exp(hf/kT) - 1} \tag{4}$$

where h is Planck's constant (6.623×10^{-34} joule-sec)

f is frequency in cps

c is the velocity of light (2.99792×10^{8} meters/sec)

k is Boltzmann's constant (1.3803×10^{-23} joule/^{o}K)

T is temperature in ^{o}K

B_f has its dimensions in w/meter^2-cps-sterad and it expresses the power emitted by a blackbody[1] at temperature T (in a transparent medium) per unit area of its surface per unit bandwidth, centered at the frequency f, per unit solid angle in the direction normal to the emitting

[1] A perfect absorber in thermodynamic equilibrium [5, pp. 93, 94; 6; 7, pp. 89-106].

surface. One should note that the units of B_f are precisely the same as the units of b. Moreover, from the geometric symmetry involved, it follows that for a blackbody source at temperature T in free space, the brightness b at the observation point P in any direction that intersects the source[2] is exactly equal to B_f. Furthermore, for hf << kT (which is certainly true for the region of the spectrum being considered and above several degrees Kelvin), one obtains the Rayleigh-Jeans approximation to Planck's formula for blackbody radiation

$$B_f = \frac{2kT}{\lambda^2} = \frac{2kf^2T}{c^2}$$

$$= 2.77 \times 10^{-23} \frac{T}{\lambda^2} \tag{5}$$

in w/meter^2-cps-sterad, with an error of about one percent in the applications encountered [5, pp. 13-14] where λ is in meters^2 and T in degrees Kelvin. Thus, for a blackbody source at temperature T in free space, the brightness b at the observation point P in any direction intersecting the source is given by

$$b = B_f = \frac{2kT_b}{\lambda^2} \tag{6}$$

where T_b is substituted for T to emphasize the relation between b and T. It is important to notice that the quantities b and T_b for a blackbody source are constant at all observation points P for which there is no absorption between the source and P; i.e., b and T_b do not depend on the inverse-square-distance law. However, the flux density at P from the blackbody source will depend on the distance between the source and P. The flux density at P from an extended source is given by

$$S = \iint_{\Omega_s} b \, d\Omega = \iint_{\Omega_s} b \sin\theta \, d\theta \, d\varphi \tag{7}$$

where Ω_s is the solid angle subtended at P by the source. If A_s is the projected area of the source normal to the direction of observation and r the distance between the source and P, and if one assumes that $A_s << r^2$, then for a blackbody source one obtains

$$S = b\Omega_s = \frac{bA_s}{r^2} = \frac{2kT_b}{\lambda^2} \frac{A_s}{r^2} \tag{8}$$

[2] There is assumed to be no absorption in the space between the source and P.

From this equation, it can be seen that the dependence of S on r enters through Ω_s, which varies with r.

By using Equation 6, one can now define the quantity T_b for any noise source (not necessarily blackbody, nor even thermal) for which the value of b is known. Since the source need not be a blackbody, the physical interpretation associated with T_b (the brightness temperature of the source) is as follows: at a given frequency, the brightness b of an extended source in a given direction can be specified in terms of a brightness temperature. This brightness temperature is defined as the temperature of an equivalent blackbody of small solid angular extent situated in the same direction in free space from which the brightness of the thermal radiation would equal that which is actually observed from the source at the point P (assuming no absorption).

For an actual blackbody source, b and T_b remain constant in any direction which intersects the source; however, this will no longer be true for an arbitrary extended source. Nevertheless, as was pointed out for the blackbody source, b and T_b are invariant with distance from P to the source, as long as the direction from P to the source remains fixed along a given direction line. The flux density received from an extended source will vary with distance if the change in distance is sufficient to significantly affect the solid angle Ω_s subtended by the source at P.

Thus, for an actual blackbody source, the above interpretation corresponds to the real physical situation, but for a graybody, pseudothermal [5], or nonthermal source, it is a convenient transformation of units because it allows the simultaneous expression of the noise radiation from all sources in terms of the simple concept of blackbody radiation which, at a given frequency, depends only on temperature.

For sources which are thermal radiators but not blackbodies, T_b can be directly calculated if their temperatures are known, and if their absorptivity (for an opaque body with a well-defined surface) or power absorption coefficient (for a partly transparent medium) are known. The calculation employs Kirchoff's law in conjunction with the Rayleigh-Jeans approximation to Planck's radiation law [6, 7], and does not necessitate knowing b which, for extraterrestrial sources, can only be obtained by measurement.

In order to use a temperature that corresponds to the flux density from discrete sources, the angular size of the source (as seen from the observation point P) must be considered. For a discrete source such as the sun, which has a finite (nonzero) angular extent, the corresponding brightness temperature is defined as the temperature of an equivalent blackbody situated in the direction of the source and having the angular size of the actual source which would yield the observed flux density. This is called "apparent temperature" to emphasize that the brightness temperature is usually not uniform over the whole disk or angular extent of the source. For

example, one defines the "apparent disk temperature" of the sun as the temperature of a blackbody having the angular size of the disk of the solar photosphere which would yield the observed flux density from the sun. The apparent temperature of a discrete source is also invariant with distance to the source, but the flux density will vary with the inverse square of the distance, as given by Equation 8.

Apparent temperature and brightness temperature (for the two kinds of sources) are specified in degrees Kelvin. As pointed out previously, temperature units are simpler and more convenient to work with than electromagnetic units, but whichever units are used, it is still necessary to specify polarization for a complete description of the incident radiation. Representation of the strength of radiation in terms of temperature is particularly convenient in the analysis of radiation of thermal origin, but the definitions given do not exclude other types of radiation. Temperature can be used simply as a representation of magnitude. Such representation has proved itself very useful in the calibration of certain receiving systems such as microwave radiometers and other extremely-low-internal-noise systems [8].

4
DERIVATION OF A GENERAL FORMULA FOR THE EFFECTIVE ANTENNA TEMPERATURE

To find the relation between the effective antenna temperature and the apparent and brightness temperatures of the various noise sources within the antenna beam, one first considers the special case of an idealized antenna of extremely small beam area Ω_a, which is focused on a distributed source of brightness temperature $T_b(\theta, \varphi)$, and whose normalized power pattern[3] $F_n(\theta, \varphi) = 0$ outside Ω_a. Since the beam area of the antenna is very small, one may consider $T_b(\theta, \varphi)$ as constant within Ω_a and equal to $T_b(\theta_0, \varphi_0) = T_b$, which is the value in the direction (θ_0, φ_0) under observation and which coincides with the direction of the polar axis of the beam. Then, for random polarization of the radiation from the noise source, the power available at the output terminals of the antenna is stated in the formula

$$P_N = \frac{kT_b}{\lambda^2} A_{em} \beta \Omega_a \text{ watts} \tag{9}$$

where A_{em} is the maximum effective aperture of the antenna. The maximum effective aperture for any antenna is

$$A_{em} = \frac{\lambda^2}{4\pi} D \text{ meters}^2 \tag{10}$$

[3]The normalized power pattern is the square of the field pattern normalized to unity at its maximum value.

where D, the antenna directivity, is defined as

$$D = 4\pi \Big/ \iint_{4\pi} F_n(\theta, \varphi)\, d\Omega \tag{11}$$

For the idealized antenna, D has the value

$$D = 4\pi/\Omega_a \tag{12}$$

where Ω_a is the beam area of the antenna (as given by the denominator of the right-hand side of Equation 11). After combining the above relations, Equations 9, 10, 11, and 12, one obtains

$$P_N = kT_b\beta \tag{13}$$

But by previous definition

$$P_N = kT_a\beta$$

Therefore, for this idealized situation,

$$T_a = T_b$$

i.e., the effective antenna temperature is exactly equal to the brightness temperature of the source.

In general, however, even a narrowbeam real antenna that is used in measuring the brightness temperature in a given direction in space will obtain only an approximation to T_b. This approximation results from varying brightness temperature over a nonconstant power pattern in the main beam and the presence of other noise sources in the side lobes. The effective antenna temperature obtained with such an antenna will be a weighted average of the normalized power pattern multiplied by the brightness temperature of all the sources seen by the antenna.[4] This process is known as smoothing the background. Thus, whenever the brightness temperature of a source is specified, it is advisable to indicate the characteristics of the antenna with which the measurement was made and to state whether the measurement has been corrected for smoothing and for the presence of other sources in the main beam and side lobes.

If an idealized antenna with $\Omega_a \leq \Omega_s$ (where Ω_s is the angular size of the source) is focused on a discrete source, the power available at the output terminals of the antenna will be

$$P_N = kT_d\beta \tag{14}$$

[4]This assertion will be proved later (Equation 35).

where T_d is the apparent temperature of the discrete source as given by

$$T_d = \frac{\lambda^2}{2k}\left(\frac{S}{\Omega_s}\right) \tag{15}$$

in which S is the total flux density from the source. This again is an instance in which the effective antenna temperature is exactly equal to the apparent temperature of the source.

Actually, the T_d in Equation 14 is the apparent temperature of that part of the source that is within the antenna beam, whereas the T_d in Equation 15 is the apparent temperature of the whole source. But, in practice, the beam areas of most antennas are greater than the solid angular sizes of the discrete sources. Therefore, it is once again useful to consider the case of an idealized antenna whose beam area is greater than the solid angular size of the discrete source upon which the beam is centered. If one assumes that the part of the sky within the beam but outside the source is at zero degrees Kelvin, then the noise power is given by

$$\begin{aligned} P_N &= \frac{kT_d}{\lambda^2}\beta A_{em}\Omega_s \\ &= kT_d\left(\frac{\Omega_s}{\Omega_a}\right)\beta \end{aligned} \tag{16}$$

Thus, the effective antenna temperature is

$$T_a = T_d\left(\frac{\Omega_s}{\Omega_a}\right) \tag{17}$$

where T_d is the apparent temperature of the whole source, as in Equation 15. It should be noted that for solar system sources, T_a will vary with the distance from the source because Ω_s will vary as the inverse square of that distance. Equation 17 can also be rewritten in terms of the flux density of the source by using Equation 15. Thus

$$T_a = \frac{\lambda^2}{2k}\left(\frac{S}{\Omega_s}\right)\left(\frac{\Omega_s}{\Omega_a}\right) = \frac{SA_{em}}{2k} = 0.362 \times 10^{23}\, SA_{em} \tag{18}$$

Equation 18 also follows directly from the relation $kT_a = \frac{SA_{em}}{2}$, in which the solid angular size of the source is not involved; thus it is valid for point sources as well.

It will now be shown that the above results for ideal antennas can be extended to some practical antennas. First, one considers a single extended source in the antenna beam. The antenna

is assumed to have a nonuniform normalized power pattern $F_n(\theta, \varphi)$ and a beamwidth narrow enough so that the brightness temperature $T_b(\theta, \varphi)$ within the beam may be considered constant and equal to T_b, the value in the direction of the polar axis of the symmetrical beam. The antenna is also assumed to have negligible side lobes. Then

$$P_N = \iint_{4\pi} \frac{kT_b(\theta, \varphi)}{\lambda^2} \beta A_e(\theta, \varphi)\, d\Omega \tag{19}$$

where $A_e(\theta, \varphi)$ is the antenna's effective aperture in the direction (θ, φ) and is given by

$$A_e(\theta, \varphi) = A_{em} F_n(\theta, \varphi) = \frac{\lambda^2}{4\pi} D F_n(\theta, \varphi) \tag{20}$$

Therefore

$$P_N = (kT_b\beta) \frac{D}{4\pi} \iint_{4\pi} F_n(\theta, \varphi)\, d\Omega$$

But

$$D = 4\pi \Big/ \iint_{4\pi} F_n(\theta, \varphi)\, d\Omega$$

Hence $P_N = kT_b\beta$, and $T_a = T_b$, as was true for the idealized antenna.

Next, one considers the situation of a similar antenna centered on a single discrete source of apparent temperature T_d, where the entire source is contained within the beam; this is the actual situation for most antennas. Then

$$\begin{aligned} P_N &= \iint_{\Omega_s} \frac{kT_d}{\lambda^2} \beta A_e(\theta, \varphi)\, d\Omega \\ &= (kT_d\beta) \frac{D}{4\pi} \iint_{\Omega_s} F_n(\theta, \varphi)\, d\Omega \end{aligned} \tag{21}$$

where Ω_s is the solid angular size of the discrete source, and where it is assumed that the part of space within the antenna beam but outside the source has a brightness temperature of zero degrees Kelvin. Equation 21 may be rewritten as

$$P_N = kT_d\beta \left[\iint_{\Omega_s} F_n(\theta, \varphi)\, d\Omega \Big/ \iint_{4\pi} F_n(\theta, \varphi)\, d\Omega \right] = kT_d\beta(\Omega_{se}/\Omega_{ae}) \tag{22}$$

where Ω_{ae} is the effective antenna-beam area and is defined by

$$\Omega_{ae} = \iint_{4\pi} F_n(\theta, \varphi)\, d\Omega \text{ sterad} \tag{23}$$

and Ω_{se} is the effective solid angular size of the source (for the particular antenna under consideration), defined by

$$\Omega_{se} = \iint_{\Omega_s} F_n(\theta, \varphi)\, d\Omega \text{ sterad} \tag{24}$$

If the solid angular size of the source is sufficiently small so that $F_n(\theta, \varphi)$ may be assumed equal to 1 within Ω_s, then $\Omega_{se} = \Omega_s$. In general, however, for a discrete source,

$$T_a = T_d\left(\frac{\Omega_{se}}{\Omega_{ae}}\right) \tag{25}$$

which is analogous to Equation 17 for the idealized antenna.

The effective antenna temperature given by Equation 25 will be smaller than that measured by a narrowbeam antenna. This occurs because the contribution from the background radiation in the main beam was neglected and the side lobes were assumed to give a negligible contribution to the effective antenna temperature. However, for most discrete sources, Equation 25 is a reasonable approximation when the antenna-beam area is not much greater than the solid angular size of the source. This holds true because the brightness temperature of the background radiation is usually much smaller than the apparent temperature of the discrete sources. The ratio Ω_{se}/Ω_{ae} has a direct physical interpretation in terms of the reciprocity relation between transmitting and receiving antennas. It represents that fraction of the total radiated power which would be radiated into the solid angle Ω_s occupied by the source if the antenna were operating as a transmitting antenna. This can be inferred directly from Equation 22.

In the most general situation, an arbitrary antenna sees a combination of discrete sources $D_1, D_2, \ldots, D_n$ and distributed sources $E_1, E_2, \ldots, E_m$ with apparent temperatures $T_d^{(1)}$, $T_d^{(2)}, \ldots, T_d^{(n)}$ and brightness temperatures $T_b^{(1)}, T_b^{(2)}, \ldots, T_b^{(m)}$, respectively, where the discrete sources subtend solid angles $\omega_1, \omega_2, \ldots, \omega_n$ and the distributed sources subtend solid angles $\Omega_1, \Omega_2, \ldots, \Omega_m$. Some of the Ω_j may be identical, others may overlap since there may be several distributed sources in a given direction all lying within the same solid angle, as for example the atmosphere and the cosmic background. Of course, $\omega_i \ll \Omega_j$. But all the ω_i are disjoint, and the ω_i and Ω_j are also disjoint, i.e., they do not overlap. The union of all the ω_i and Ω_j gives the whole 4π sterad of the sphere in which the noise sources are distributed.

with respect to a fixed azimuth- and elevation-angle coordinate system (θ, φ). If $T(\theta, \varphi)$ denotes the brightness temperature in the direction (θ, φ) from all the distributed noise sources in that direction, or the apparent temperature of the particular discrete source in that direction, whichever is the actual situation in the direction (θ, φ), then the total available noise power at the antenna output, from all the sources, is

$$P_N = k\beta \frac{D}{4\pi} \iint_{4\pi} T(\theta, \varphi) F_n(\theta, \varphi)\, d\Omega \tag{26}$$

where D is given by Equation 11. The contribution to P_N from a single distributed source E_j is given by

$$P_N(E_j) = k\beta \frac{D}{4\pi} \iint_{\Omega_j} T_b^{(j)}(\theta, \varphi) F_n(\theta, \varphi)\, d\Omega \quad (j = 1, 2, \ldots, m) \tag{27}$$

and from a single discrete source D_i by

$$P_N(D_i) = k\beta \frac{D}{4\pi} \iint_{\omega_i} T_d^{(i)} F_n(\theta, \varphi)\, d\Omega \quad (i = 1, \ldots, n) \tag{28}$$

Since the antenna is a linear power device and since the radio noise is incoherent, one obtains

$$P_N = \sum_{j=1}^{m} P_N(E_j) + \sum_{i=1}^{n} P_N(D_i) \tag{29}$$

Upon denoting by d_i the value of $\frac{D}{4\pi} \iint_{\omega_i} F_n(\theta, \varphi)\, d\Omega$, which is a constant representing the fraction of total power that would be radiated by the antenna into the solid angle ω_i if the antenna were operating as a transmitting antenna, Equation 28 becomes

$$P_N(D_i) = d_i\left(kT_d^{(i)}\beta\right) \tag{30}$$

where d_i satisfies the inequality $0 \leq d_i \leq 1$.

Moreover, if the solid angles Ω_j are fairly small (which is true for a narrowbeam antenna), then one may approximate the varying brightness $T_b^{(j)}(\theta, \varphi)$ within Ω_j by the mean value

$$\overline{T}_b^{(j)} = \frac{1}{\Omega_j} \iint_{\Omega_j} T_b^{(j)}(\theta, \varphi)\, d\Omega \tag{31}$$

to obtain the approximation in Equation 27

$$P_N(E_j) = c_j\left(k\overline{T}_b^{(j)}\beta\right) \tag{32}$$

where

$$c_j = \frac{D}{4\pi} \iint_{\Omega_j} F_n(\theta, \varphi)\, d\Omega \tag{33}$$

and c_j has the same physical interpretation and numerical bounds as were defined previously for d_i. Then, upon combining Equations 29, 30, and 32, one obtains

$$\begin{aligned} P_N = k\beta T_a &= \sum_{i=1}^{n} d_i \left[k\beta T_d^{(i)}\right] + \sum_{j=1}^{m} c_j \left[k\beta \overline{T}_b^{(j)}\right] \\ &= k\beta \left(\sum_{i=1}^{n} d_i T_d^{(i)} + \sum_{j=1}^{m} c_j \overline{T}_b^{(j)} \right) \end{aligned} \tag{34}$$

Equation 34 shows that the effective antenna temperature is

$$T_a = \sum_{i=1}^{n} d_i T_d^{(i)} + \sum_{j=1}^{m} c_j \overline{T}_b^{(j)} \tag{35}$$

Thus, it follows that the effective antenna temperature is equal to the sum of a weighted average of the apparent temperatures of the discrete sources and a weighted average of the mean brightness temperatures of the distributed sources. The weighting factors d_i and c_j are equal to the fraction of total power that would be radiated into the solid angles ω_i and Ω_j, respectively, if the antenna were operating as a transmitting antenna.

The above analysis, which holds only for lossless antennas, shows that the effective antenna temperature depends only on the brightness and apparent temperatures of the sources, on the antenna directivity, and on the spatial distribution of the sources with respect to the normalized power pattern of the antenna; it is entirely unrelated to the actual temperature of the antenna material itself.

However, if the antenna is not lossless, it will contribute thermal radiation in addition to its action as an attenuator. If one supposes that the temperature of the antenna matter is T_0 and that the efficiency of the antenna is η, then by the principle of detailed balancing of radiation [5, pp. 21-24], it follows that the effective antenna temperature T'_a for a lossy antenna is given by

$$T'_a = \eta T_a + (1 - \eta) T_0 \tag{36}$$

where T_a is the effective antenna temperature that would be observed by a lossless antenna having the same normalized power pattern and the same directivity D as the lossy antenna (T_a is

given by Equation 35). It can be seen from Equation 36 that whenever $T_0 > T_a$, then $T'_a > T_a$; hence, the net effect of the antenna losses is to contribute excess noise.

5
RADIO NOISE IN THE 0.1- TO 40.0-Gc BAND

Now that the relation between effective antenna temperature and the various noise sources within the antenna beam has been established, one can examine the experimental and empirical data available on the sources themselves and attempt to properly interpret these data for the purpose of numerical computation of the effective antenna temperature.

The various noise sources in the universe that may contribute noise to the antenna may be classified as (1) terrestrial sources (earth and earth's atmosphere); (2) solar system sources (planets, moon, and sun); and (3) cosmic sources (galactic and extragalactic).

The spatial distribution of cosmic radio noise consists of an unresolved continuous background radiation varying smoothly over the entire celestial sphere together with numerous discrete sources such as radio galaxies and various localized sources within the Milky Way. The cosmic background radiation is strongest in directions pointing toward the galactic plane, with the peak occurring in the direction of the galactic center. Outside the galactic plane, the cosmic background is extremely weak. It is not known presently whether this cosmic background is in reality a spatially smooth distribution from extended sources or is actually a superposition of a multitude of faint discrete sources which cannot be resolved with the presently available radio telescopes.

Several thousand discrete cosmic radio sources have now been discovered, some of which have been identified with relatively near objects in our own galaxy such as emission nebulae composed of intensely hot interstellar masses of gas and other nebulae that are the remnants of supernovas. Other discrete cosmic radio sources, like Cygnus A, have been identified with extragalactic objects, and there is now considerable evidence that the majority of discrete cosmic radio sources are associated with external galaxies. Approximately 100 discrete radio sources have been identified with visible galaxies. Since radio sources as intense as Cygnus A could be detected by radio telescopes even if they were far beyond the range of present optical telescopes, apparently some of the radio sources not yet associated with visible objects are too remote to be seen optically. Both the cosmic background and the discrete sources have a continuous spectrum, the only exception being the 1420-Mc cold, neutral, atomic-hydrogen line radiation from the galactic plane, which fails to show a pronounced maximum in the direction of the galactic center. The continuous spectra of the spatially smooth cosmic background and

the continuous spectra of the radiation from most of the discrete sources show a rapid decrease of brightness temperature and apparent temperature, respectively, as the frequency increases. These spectra are nonthermal; i.e., they are incompatible with possible kinetic temperatures and Maxwellian velocity distributions of the elementary radiating particles in the sources exhibiting these emission spectra.

The waveform of the cosmic background radiation and that from the discrete sources is similar to random noise. The polarization appears to be random, with minor exceptions (minor in the sense of this paper, but not from the point of view of radio astronomy). The mean cosmic brightness from an extended part of the sky does not show observable fluctuation at the earth's surface, except at low frequencies approaching the critical frequency of the ionosphere. But the radiation from discrete sources shows marked fluctuations at the earth's surface, both in intensity and direction. These fluctuations are analogous to the twinkling of stars, but are caused primarily by the nonhomogeneity of the ionosphere rather than of the lower atmosphere. These fluctuations are significant only at the lower radio frequencies [5, 8, 9].

5.1. TERRESTRIAL RADIO NOISE

5.1.1. RADIO NOISE FROM THE EARTH. Any object which absorbs radiation at a given frequency f will emit radiation at the same frequency as a result of thermal agitation. When the object is a purely thermal radiator, the limit of this radiation at the frequency f and temperature T is that given by Planck's radiation law for a blackbody. In general, the emission at the frequency f will be less than that for a blackbody at the same temperature, and depends on the absorptivity a(f) at the frequency f. At a temperature T, a body which is a purely thermal radiator will have a brightness temperature expressed by

$$T_b = a(f)T \tag{37}$$

Equation 37 is correct only when the object is in thermodynamic equilibrium, but it is still valid for more general conditions [7]. The earth is a thermal emitter, at an average temperature of 288°K (15°C), but it is not a blackbody. It approaches a blackbody in the millimeter and infrared parts of the spectrum and at K-band microwave frequencies. If the side lobes of an antenna that is pointed toward the sky accept radiation from the earth, then to calculate the earth's contribution to the effective antenna temperature, one first calculates the mean brightness temperature over the surface area of the earth that is seen by the side lobes by using Equations 31 and 37, then one computes the appropriate weighting factor c_j in Equation 33, and, finally, one uses Equation 32.

5.1.2. RADIO NOISE FROM THE ATMOSPHERE. Noise also originates in the earth's atmosphere, primarily in the troposphere, because of absorption of radio and microwave energy

by oxygen, water vapor, and rain. Thus, an antenna that is located on the surface of the earth and is pointed toward the sky is surrounded by an absorbing atmosphere that emits thermal radiation. Similarly, an antenna located in aerospace, part of whose main beam (or side lobes) sees the atmosphere, will receive noise from that part of the atmosphere intercepted by the main beam (or side lobes).

D. C. Hogg [10] has calculated the brightness temperature of the atmosphere as a function of zenith angle for the 0.5- to 40.0-Gc frequency band for a point P on the earth's surface. His results are shown in Figure 1. Experimental evidence [4, 10, 11, 12] indicates that these results are quite accurate for the atmospheric conditions they represent, and much confidence in them has been expressed in the literature.

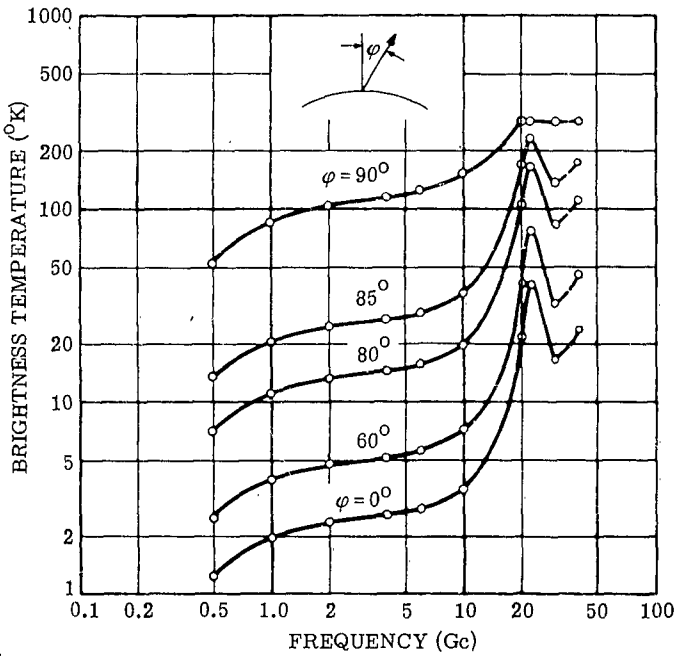

FIGURE 1. BRIGHTNESS TEMPERATURE ON THE EARTH FROM OXYGEN AND WATER VAPOR IN THE ATMOSPHERE [10]

Absorption (and therefore emission) of radio waves by the atmosphere depends on the temperature, pressure, and water vapor content of the air. The curves of Figure 1 are based on an atmospheric model shown in Figure 2. This model represents typical summer conditions that

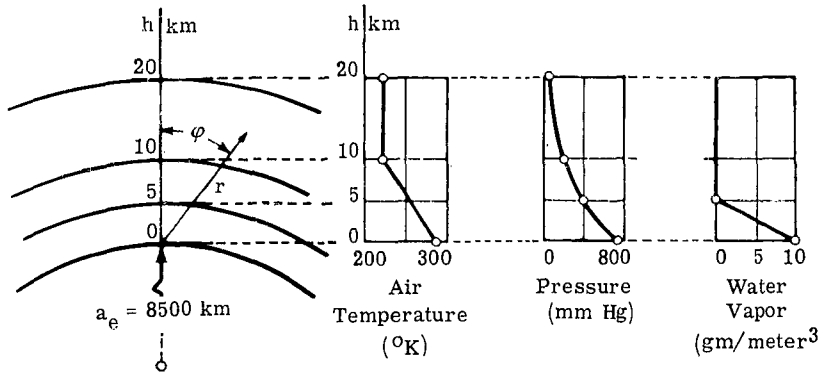

FIGURE 2. MODEL OF THE RADIO EARTH AND ITS ATMOSPHERE [10]

exist in the first 20 km of the atmosphere. The dependence of temperature and pressure on height is essentially that of the International Standard Atmosphere, and the water vapor content is assumed to vary linearly from 10 gm/meter^3 at the earth's surface to zero at a height of 5 km. The actual water vapor content that can prevail on the surface of the earth in temperate climates may vary from 1 gm/meter^3 in winter to 20 gm/meter^3 in summer. Figure 2 also shows the spherical earth with a radio radius a_e of 8500 km used in the calculations. On the earth's surface, the brightness temperature of the atmosphere is given by the formula [13],

$$T_b = \int_0^\infty \alpha\, T \exp\left(-\int_0^r \alpha\, dr\right) dr \qquad (38)$$

where α and T are, respectively, the power absorption coefficient and temperature in degrees Kelvin at a point (r, φ) shown in Figure 2. For Equation 38, α is a function of r, φ, temperature, pressure (which is equivalent to oxygen content), and water vapor content; consequently, $\alpha = \alpha_o + \alpha_w$ where α_o represents absorption due to oxygen and α_w due to water vapor. Equation 38 is analogous to Equation 22 for the brightness temperature of the earth except for the factor $\exp\left(-\int_0^r \alpha\, dr\right)$, which represents the attenuation of the radiation from an incremental volume element of the atmosphere as the radiation travels through the rest of the atmosphere to the surface of the earth.

The absorption coefficient α_o, in the radio and microwave bands, is a result of magnetic dipole resonances of the oxygen molecules at about 60 Gc. Because of pressure broadening of the resonance lines, the tails of these lines extend through the microwave region and cause most of the absorption and antenna noise. Brightness temperatures caused by oxygen, i.e., using α_o

instead of α in Equation 38, also calculated by D. C. Hogg, are shown in Figure 3. These are also subject to the atmospheric conditions shown in Figure 2.

In the radio and microwave bands, the absorption coefficient α_w caused by water vapor consists of a sum of two terms: $\alpha_w = \alpha_{w1} + \alpha_{w2}$, where α_{w1} is the contribution to α_w introduced by an electric dipole resonance near 22.5 Gc with its associated pressure broadening, and α_{w2} arises as a result of strong water vapor resonances in the infrared band, since the tails of these resonance lines are significant even in the microwave region. Brightness temperatures caused by water vapor alone are shown in Figure 4, also from [10]. Figure 5 shows the one-way total attenuation through the atmosphere—a result which is incidental to Hogg's calculation of the atmospheric brightness temperatures, but which is, indeed, very useful in itself.

The effects of rain and water vapor content on the brightness temperature of the atmosphere have been studied by Hogg and Semplak [12]. They give upper and lower bounds on the brightness temperature of the atmosphere at microwave frequencies that may be expected as a result of variation of water vapor content. Their measurements of the effect of rain on the brightness

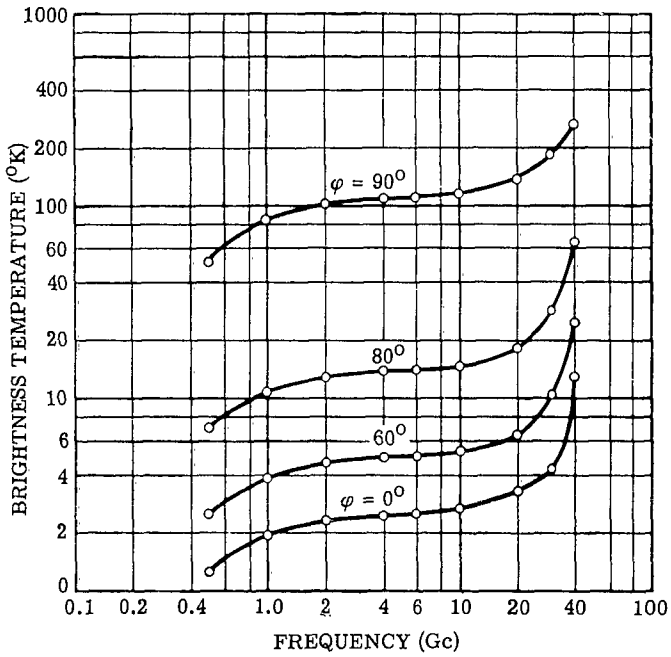

FIGURE 3. BRIGHTNESS TEMPERATURE ON THE EARTH FROM OXYGEN IN THE ATMOSPHERE [10]

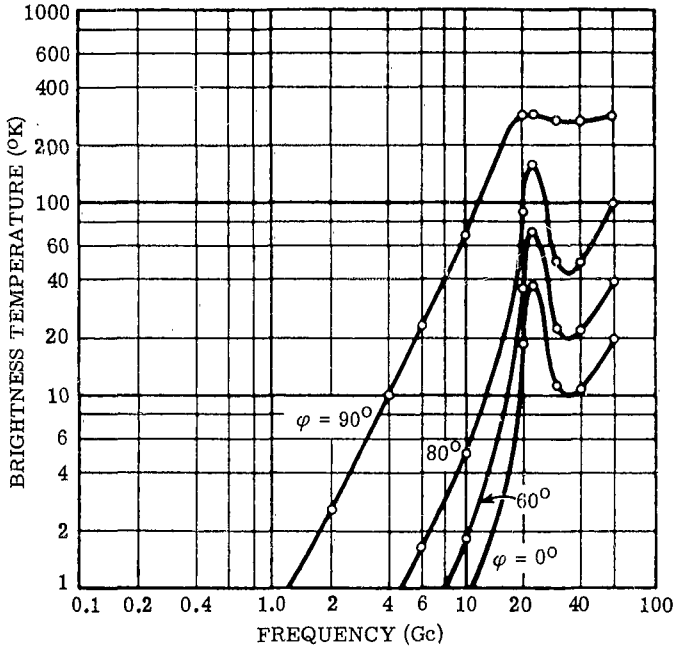

FIGURE 4. BRIGHTNESS TEMPERATURE ON THE EARTH FROM WATER VAPOR IN THE ATMOSPHERE [10]

temperature indicate that at 6 Gc rain can increase the brightness temperature of the atmosphere by as much as 17 db, even with the antenna beam in the favorable zenith position. Comprehensive data for the effect of rain on the atmospheric brightness temperature are not available, and it is difficult to interpret even the available data because rain is not radially stratified and the distribution of condensed water vapor with altitude depends on many meteorological conditions; in short, there are too many variables. Furthermore, the experiments of Hogg and Semplak have shown that there is no significant correlation between measured brightness temperature and ground rain rate at the measuring station.

The above discussion and the brightness temperatures quoted refer to an observation point on the surface of the earth. If the antenna is located at some point P in aerospace, a number of different considerations enter. The geometry involved here is depicted in Figure 6. In all directions outside the cone determined by the lines PA and PD, the atmosphere will not contribute any noise, since the essential part of the atmosphere is confined to the interior of this cone. In the interior of this cone the noise received from the atmosphere will vary from its minimum

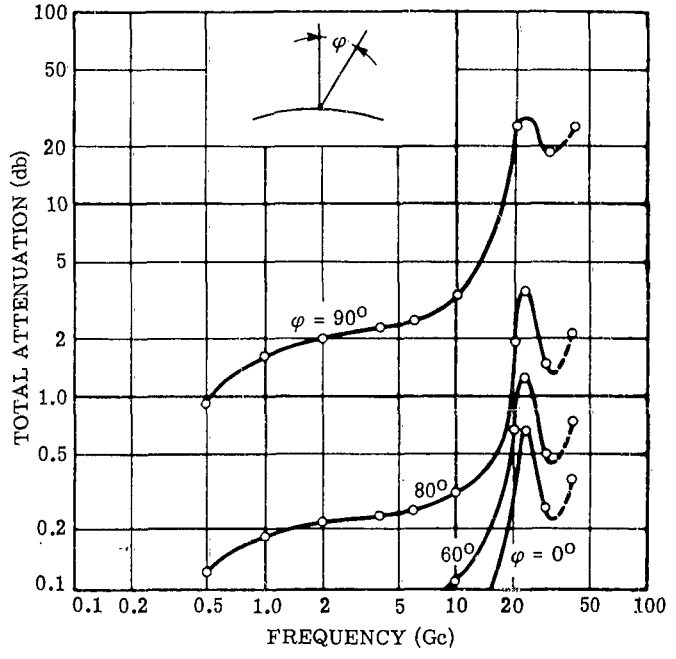

FIGURE 5. ONE-WAY TOTAL ATTENUATION THROUGH THE ATMOSPHERE BY OXYGEN AND WATER VAPOR [10]

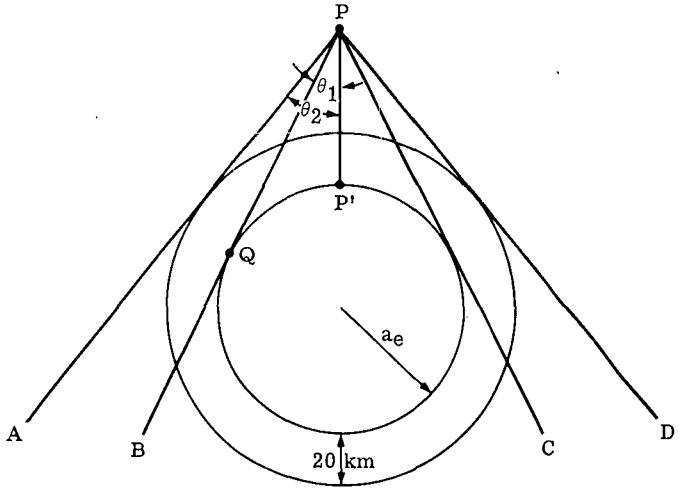

FIGURE 6. GEOMETRY INVOLVED IN RADIO NOISE RECEIVED FROM THE ATMOSPHERE AT AN OBSERVATION POINT P IN AEROSPACE

value in the directions PA and PD (minimum path length through atmosphere) to its maximum value in the directions PB and PC (maximum path length). As the direction changes from PA to PP', T_b increases to its maximum value as the direction PB is approached, then T_b decreases sharply as the direction PB is passed, and continues to decrease to its minimum value in the direction PP'. It is not possible to calculate the atmospheric brightness temperatures at P from Hogg's values for points on the earth's surface because of the nonhomogeneity of the atmosphere and because of the different paths through the atmosphere that are encountered in this case, even if one makes the reasonable assumption that Hogg's atmospheric model is valid when viewed from above the atmosphere.[5] Of course, the total one-way attenuation is the same in this case as long as the path considered is the same as that from a given point on the earth's surface. However, reasonable bounds on T_b can be determined for a point P in aerospace from Hogg's values for the earth's surface. A detailed analysis of the functional behavior of the variables involved in Equation 38 shows that the brightness temperature of the atmosphere at P when observed in the direction PP' is approximately equal to (and, at most, equal to) the brightness temperature at P' when observed in the direction P'P. A similar result is valid for directions θ within the angle θ_1, but not in the direction PB. The direction PB indicates the longest possible path through the atmosphere, so that the highest brightness temperature caused by the atmosphere observable at P is associated with this direction. The expression

$$(T_b)_{PB} \approx (T_b)_{90^o} (1 + A_{90^o}) \tag{39}$$

gives a good approximation to the brightness temperature $(T_b)_{PB}$ in the direction PB. In Equation 39, A_{90^o} is the fractional one-way total attenuation through the atmosphere at $\varphi = 90^o$ (Figure 5) and $(T_b)_{90^o}$ is the brightness temperature on the earth at $\varphi = 90^o$ (Figure 1). The brightness temperature will then decrease continuously from $(T_b)_{PB}$ to zero as the direction of observation changes from PB to PA, respectively.

In addition to receiving noise from the atmosphere, an antenna located at a point P in aerospace will also receive thermal noise from the earth whenever the main beam (or side lobes) sees the earth. In this situation, the brightness temperature caused by the earth at P will be that given by Equation 37, diminished by the total one-way attenuation through that path in the atmosphere in the particular direction under consideration. Hence, the brightness temperature due to the earth at P in a direction that meets the earth is given by

$$T_b = a(f)AT \tag{40}$$

[5] The brightness temperature in the direction PP' turns out to be $(T_b)_{PP'} = \exp\left(-\int_0^\infty \alpha\, dr\right)\int_0^\infty \alpha\, T \exp\left(\int_0^r \alpha\, dr\right) dr$. Compare with $(T_b)_{P'P}$ as given by Equation 38.

where a(f) and T are the same as in Equation 37, and A is the fractional one-way total attenuation through the atmosphere at an angle φ (Figure 5) corresponding to the direction of observation at P.

5.2. PLANETARY RADIO NOISE

All the planets emit radio noise by ordinary thermal radiation, as the earth does, but some of the planets also emit radio noise of a nonthermal character. The planets Venus, Mars, Jupiter, and Saturn have all been detected, and a number of measurements of the intensity of their noise radiation have been obtained by C. H. Mayer and others [14, 15]. Strong bursts of radio noise from Jupiter at 22 Mc were discovered in 1955 by B. F. Burke and K. L. Franklin [16, 17] and subsequently confirmed by several other observers. Sporadic radio-noise bursts from Venus have also been reported. The origin of this impulsive nonthermal radiation is unknown, but it apparently decreases rapidly with increasing frequency. The observable sporadic Jovian spectrum appears to lie between the terrestrial ionospheric cutoff frequency and a frequency of about 30 Mc [17]. The Jovian noise storms range in duration from a few seconds to several hours and the percentage of total observation time during which Jupiter was active ranges from 0.1% to 22% at the various frequencies observed. Furthermore, very intense microwave radiation from Jupiter has recently been detected in the frequency band 0.44 to 10 Gc. This radiation, though not of the same nature as the sporadic bursts, cannot be interpreted as thermal radiation since this would imply unrealistically high planetary kinetic temperatures on the order of 50,000°K [15, 17].

Table I lists the apparent disk temperatures, in degrees Kelvin, as a function of frequency for the planets Venus, Jupiter, and Mars. For Venus and Mars the apparent temperatures represent essentially thermal noise radiation, while for Jupiter the noise radiation is essentially of nonthermal origin at the lower frequencies indicated. The accuracies for these values of apparent temperature are generally low, the estimated mean errors ranging from ±15% to ±50% [14, 15, 18].

5.3. SOLAR RADIO NOISE

The sun is an intense radio-noise source whose radio-frequency spectrum shows great complexity and variability. The radio emission from the sun is usually divided, in a perhaps arbitrary manner, into two principal categories: (1) radiation from the "quiet sun," and (2) radiation from the "disturbed" or "active" sun. The radiation from the quiet sun is the lowest level of background thermal emission from the solar atmosphere; the radiation from the disturbed sun is that which originates in localized active areas in the solar atmosphere. At optical frequencies and in the millimeter band (above 30 Gc), the radiation is nearly that from a blackbody at 6000°K.

TABLE I. PLANETARY RADIO NOISE IN THE MICROWAVE FREQUENCY BAND

PLANET	FREQUENCY (Gc)	APPARENT* DISK TEMPERATURE (^{o}K)
Venus:	35	410
	9.5	590
	3	580
Mars:	9.5	218
Jupiter:	9.5	145
	2.9	640
	1.4	3000
	.97	5500
	.44	50,000

*The apparent temperatures are based on the average solid angle subtended by the planets. The quoted values have been corrected for antenna pointing errors and for atmospheric absorption.

For frequencies below 30 Gc, however, the apparent temperature of the quiet sun is much greater than would be expected from a blackbody at 6000^{o}K. The apparent temperature of the quiet sun varies from about 6000^{o}K at 30 Gc to about 7×10^{5}^{o}K at 0.3 Gc. Figure 7 is a plot of the apparent temperature of the quiet sun [5, 19]. Moreover, at frequencies below 30 Gc, significant time-dependent increases in the radiation become apparent. In the frequency band between about 0.5 Gc and 15 Gc there is a general enhancement above the quiet sun component of continuum radiation. The enhanced continuum radiation is about double the value of that from the quiet sun [17, 18], with a periodicity of weeks or months which is related to the total area occupied by sunspots on the solar disk. In this frequency band solar flares are also responsible for moderately strong sporadic outbursts of radiation, lasting on the order of a few minutes. In the frequency band above about 0.25 Gc the background continuum radiation from the sun (quiet sun component plus continuum enhancement) remains essentially constant for a considerable fraction of the time, but violent disturbances are observed, especially near the maximum of the sunspot cycle [5, 17, 18, 20]. The so-called "noise storms," consisting of trains of bursts coupled with an enhancement of the background continuum radiation, may last for hours or even days and are characterized by strong circular polarization.

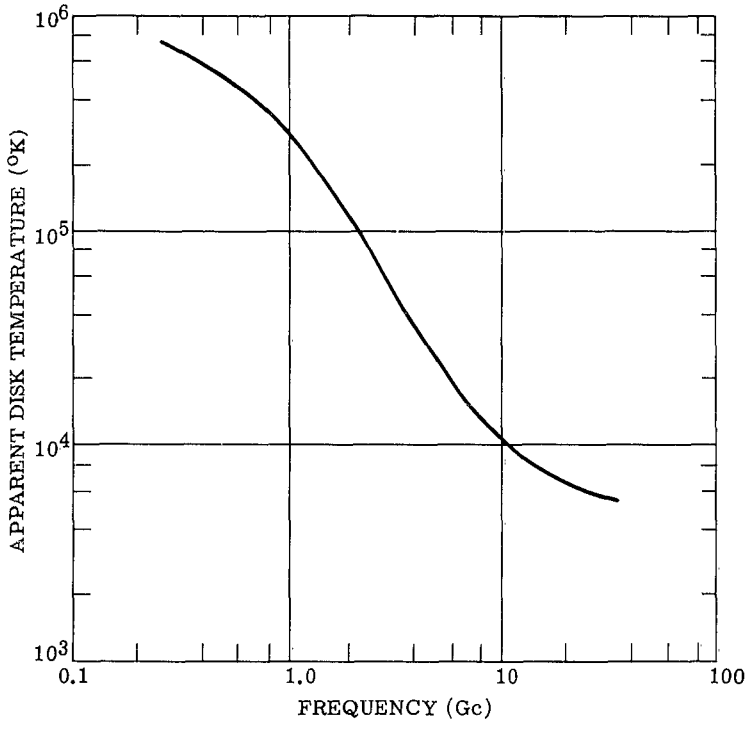

FIGURE 7. APPARENT DISK TEMPERATURE OF THE "QUIET" RADIO SUN [19]

Solar radio-wave disturbances called "outbursts," which have durations on the order of minutes, are associated with solar flares, and may reach intensities millions of times the intensity of the quiet sun and involve almost the entire radio band below 3 Gc. "Isolated bursts" ranging in duration from about 5 to 10 seconds are very common.

The complexity of the solar radio emission is responsible for the great difficulty in compiling statistics on the percentage of time that the sun is in a disturbed radio state at any given frequency. The radio disturbances are, of course, more frequent and more intense near sunspot maximum.

Thus it is seen that the apparent temperature due to the quiet sun is the minimum apparent temperature that can be observed, and that extremely high apparent temperatures may be observed under disturbed radio-sun conditions for limited durations.

5.4. LUNAR RADIO NOISE

The radio emission from the moon is of thermal origin. Very accurate measurements by Gibson [21] show that the apparent temperature of the moon at 35 Gc varies with lunar phase from 215°K to 145°K, the maximum occurring between full moon and third quarter, and the minimum between new moon and first quarter. These values are corrected for atmospheric absorption, which is very high at 35 Gc as can be seen from Figure 5. If the moon were a graybody, then one would expect its apparent temperature to remain constant with varying frequency. But the moon, like the earth, is not a graybody over the entire radio-frequency spectrum, and its apparent temperature will decrease as the frequency decreases. It is for this reason, and because extremely small beam areas can be obtained at K_a-band frequencies, that measurements of the lunar thermal radiation have been undertaken primarily at K_a-band frequencies.

(It should be noted that whenever brightness temperatures and apparent temperatures have been corrected for atmospheric effects, the corrected temperatures are those that would be observed outside the earth's atmosphere, for example, in aerospace. To calculate the corresponding temperatures that would be observed at the earth's surface, one must multiply the corrected temperatures by the fractional one-way total attenuation caused by the atmosphere. However, at frequencies between the ionospheric cutoff frequency and 5 Gc, the corrected and uncorrected values of temperature will differ very little.)

5.5. COSMIC RADIO NOISE

5.5.1. THE COSMIC RADIO-NOISE BACKGROUND. The primary features of cosmic radio noise, such as its dependence on frequency, time, space, and polarization have been discussed previously for both the cosmic background emission and emission from discrete cosmic sources. The spatial distribution and the frequency dependence of cosmic radio noise will now be considered in greater detail.

The data available on the spatially continuous cosmic background is in the form of radio surveys or maps of the celestial sphere. The radio maps as given by the original observers appear in various coordinate systems (celestial, galactic), in various projections of these coordinate systems (Mercator, Aitoff, and stereographic), and in a number of units (effective antenna temperature, brightness temperature above the "coldest" parts of the sky, and brightness). Such a radio map consists of a plot of contours of constant radio-noise levels (isophotes) on a projected galactic or celestial coordinate system, at a constant frequency. Radio maps of the sky have been made at frequencies ranging from several megacycles to about 1.3 Gc. The upper frequency limit on these surveys is a consequence of the very low brightness temperatures above 1 Gc over most of the sky except in two localized regions, the galactic nucleus and a neighboring region along the

galactic equator, which may have brightness temperatures slightly above the limit of sensitivity of the most sensitive radio telescopes. The most comprehensive of the surveys published to date have been collected and analyzed by a number of researchers [8, 18, 22, 23]. The radio map shown in Figure 8 is taken from Ko [22] and gives the cosmic radio background at 0.25 Gc. This map is in galactic coordinates under Aitoff projection.

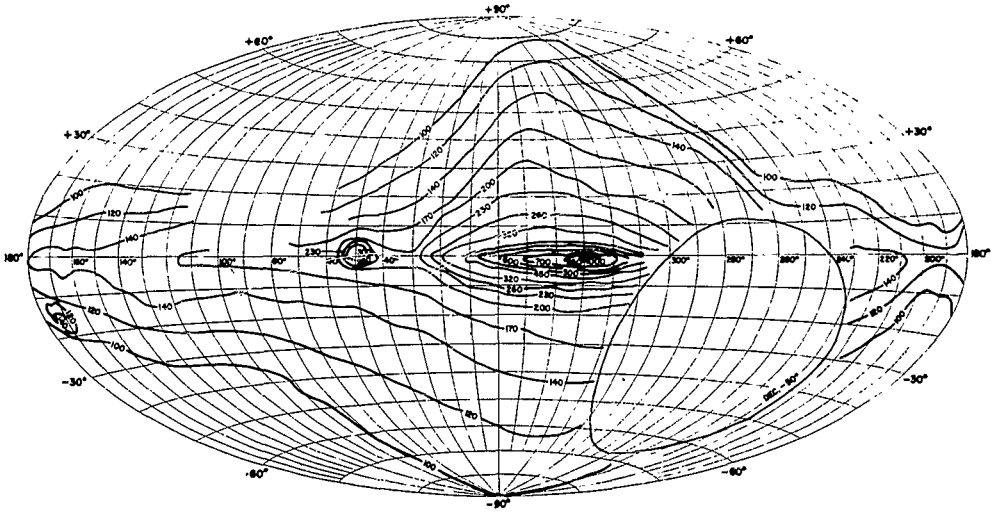

FIGURE 8. COSMIC BACKGROUND RADIO-NOISE SURVEY AT 0.25 Gc [22]

From Figure 8 it can be seen that the radio isophotes are concentrated toward the galactic equator (latitude = 0^{o}), which defines the galactic plane. This means that the brightness temperature increases as the galactic plane is approached. But as the galactic poles are approached, the brightness temperature decreases to a minimum value. If one plots T_b as a function of longitude along the galactic equator, it can be seen that as the galactic center is approached T_b increases slowly at first and then peaks sharply in the neighborhood of the galactic center or nucleus (in the constellation Sagittarius).

Thus, the general form of the radio isophotes is closely related to the shape of the galaxy and indicates that the major contribution to the cosmic radio background is caused by radiation from widely distributed ionized interstellar gas clouds or other sources widely distributed throughout our galaxy, or possibly by both. The galactic radiation is superimposed on an iso-

tropic component corresponding to the minimum brightness temperature observed in the neighborhood of the galactic poles. The isotropic component apparently has its origin in a spherical halo enveloping our galaxy, or in a spherical distribution of distant galaxies and clusters of galaxies, or perhaps both [5, 8, 17, 22].

Ko [22] and Kraus and Ko [8] have collected and analyzed eight of the most complete and reliable radio surveys of the cosmic background and several localized surveys from the neighborhood of the galactic nucleus. The eight extensive surveys cover frequencies ranging from 0.064 to 0.910 Gc. All these surveys are presented in celestial equatorial coordinates (right ascension or hour angle α, and declination δ), with absolute brightness temperature in degrees Kelvin. All are to the same scale under Mercator projection, with the different beamwidths indicated on each chart, in order to facilitate intercomparison and interpolation between the maps. These radio maps reveal the same principal features, as far as gross spatial distribution of the cosmic background is concerned, as the 0.25-Gc survey by Kraus and Ko, so that the previous conclusions for the 0.25-Gc radio map are valid for these surveys as well. The maximum and minimum brightness temperatures (corresponding to the galactic nucleus and the galactic poles, respectively) are given in Table II, and are plotted in Figure 9. These include an extra point taken from 18.3-Mc data in the neighborhood of the galactic center [8]. The accuracy of the

TABLE II. MEASURED VALUES OF BRIGHTNESS TEMPERATURE OF COSMIC BACKGROUND IN THE DIRECTION OF THE GALACTIC CENTER (MAXIMUM) AND IN THE DIRECTION OF THE GALACTIC POLE (MINIMUM)*

Frequency (Gc)	T_b in the Direction of the Galactic Center (^oK)	T_b in the Direction of the Galactic Pole (^oK)	Half-Power Beamwidth of Antenna Used in the Measurement
0.0183	300,000	60,000	$17^o \times 17^o$
0.064	20,000	2,000	$13^o \times 14^o$
0.081	14,000	1,000	$2^o \times 15^o$
0.1	2,850	550	$17^o \times 17^o$
0.160	1,650	230	$12^o \times 12^o$
0.250	1,000	90	$1.2^o \times 8^o$
0.480	180	35	$3^o \times 3^o$
0.600	280	8	$3.3^o \times 3.3^o$
0.910	80	1.5	$3.5^o \times 3.5^o$

*From various surveys selected and interpreted by Ko [22] and Kraus and Ko [8].

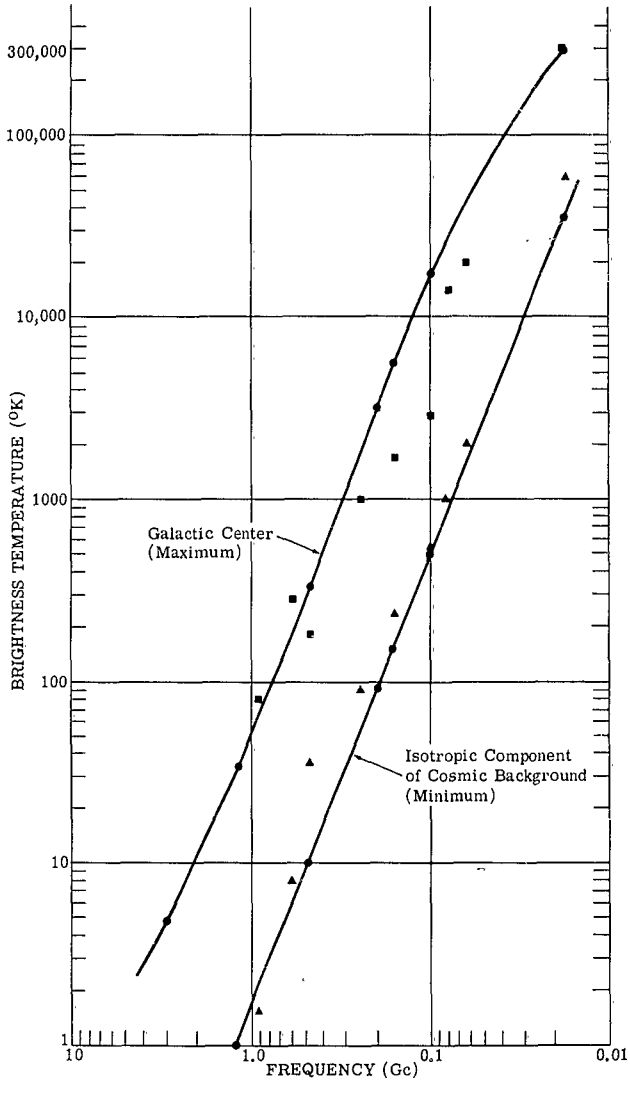

FIGURE 9. COSMIC BACKGROUND RADIO NOISE — MAXIMUM AND MINIMUM VALUES OF MEASURED AND CALCULATED BRIGHTNESS TEMPERATURE

- Calculated brightness temperature (Brown and Hazard Model) [23]
- Brightness temperature in the direction of the galactic center (maximum) [8, 22]
- Brightness temperature in the direction of the galactic pole (minimum) [8, 22]

values quoted in Table II is not high; the accuracy of the absolute temperatures on the radio maps from which Table II was constructed is estimated by Kraus and Ko to vary from ±25% to ±50%. However, the relative accuracy of each map from which these values were taken, or the accuracy of the brightness temperature of one portion of the sky relative to another on a single map, is in the range of perhaps 5 to 20%; i.e., the internal accuracy of a single radio map is much better than the overall accuracy of all the maps, or the external accuracy. It is necessary to know the sources of error in making a survey of the radio sky in order to appreciate the difficulty of obtaining high accuracy.

The first problem is that of inadequate resolution. In measuring the brightness temperature variation over the celestial sphere, from which the radio maps are prepared, the smallest measurable temperature difference (which is related to the smallest measurable increment of the effective antenna temperature) is determined by the receiver sensitivity, and the measurable detail depends on the antenna resolving power. Since no practical antenna has an infinitely sharp beam, the true brightness distribution is blurred, so that the observed brightness distribution is smoother than the true one. Detailed structure of the true brightness distribution that is less than the half-power beamwidth is lost by the smoothing process of the antenna, and cannot be restored by subsequent data processing techniques, called "sharpening" [5, 8, 22]. Thus the lower-frequency surveys (corresponding to the larger beamwidths of antennas employed) (see Table II) show much less detail than the higher-frequency surveys. In particular, this is even more pronounced in the neighborhood of the galactic nucleus, since it is known that here the brightness temperature profile rises very steeply. Hence, measurements are likely to be less accurate in the neighborhood of the galactic equator (and especially the galactic center) than anywhere else in the sky.

Second, minor lobes of the antenna power pattern may have an appreciable effect on the observed effective antenna temperature of the radio telescope. Thus if the main beam is focused on a region of the sky of low brightness temperature, say $20^{\circ}K$, but several of the side lobes are directed at regions of much higher brightness temperature or at the earth, then the observed effective antenna temperature of the radio telescope will be a weighted mean (see Equation 35) which is greater than $20^{\circ}K$. Most directional antennas have about 70% of their beam area in the main beam and 30% in the minor lobes. Therefore it is necessary to make corrections. Such corrections also have inherent errors, but they are smaller than the errors involved in uncorrected data.

A third, very important factor is the limited receiver sensitivity at the higher frequencies (above about 0.2 Gc) at which the brightness temperature of the coldest part of the sky is so low that any accurate measurement of it is extremely difficult. Hence many surveys at higher fre-

quencies give the results not in terms of absolute brightness temperature, but in terms of a relative temperature measured above the base temperature corresponding to the coldest part of the sky, without any accurate determination of this reference temperature.

Thus, for the 0.25-Gc survey by Kraus and Ko, measurements indicated that this base temperature was $80^{\circ}K \pm 30^{\circ}K$. For the eight surveys summarized, Kraus and Ko estimated the absolute base temperature by means of a study of all the available measurements of the brightness temperature of the galactic poles at the various frequencies, but the accuracy of this estimate is generally low.

Furthermore, the determination of absolute brightness temperature, even at the lower frequencies, requires a very accurate knowledge of the antenna power pattern and a very reliable method for noise power calibration. But accurate determination of the antenna power pattern for large radio telescopes is very difficult. These considerations should be borne in mind in comparisons of radio maps by different observers, at different frequencies, and with different beamwidths.

In addition to the sources of error discussed above, the discrete radio sources also contribute to the antenna temperature of the radio telescope that is used in making a survey of the cosmic radio background. The contribution from discrete cosmic sources is usually negligible for low-directivity (widebeam) antennas, as may be seen from Equations 18 and 25, since all the known discrete cosmic sources (excluding solar system sources) have flux densities which are much less than the contribution from the cosmic background radiation within the antenna beam. But for antennas of high directivity, the contribution from discrete sources to the effective antenna temperature of the radio telescope, as compared with the contribution from the cosmic background within the antenna beam, becomes increasingly significant. The cosmic discrete sources are discussed in Section 5.5.2.

In the 0.250-Gc radio map by Kraus and Ko the humps (caused by radio stars) on the profiles (effective antenna temperature vs. right ascension for a particular declination) were removed in calculating the brightness temperature caused by the cosmic background radiation.

For further details on the spatial distribution and frequency dependence of the cosmic radio background, and on the relation of the spatial distribution to the general shape of our galaxy and to certain localized structural complexes within the galaxy, the reader is referred to other available literature [5, 8, 22].

In 1953, Brown and Hazard [23], on the basis of radio surveys of the cosmic background available at that time, postulated a model of the galaxy from which the radio galaxy was derived theoretically; i.e., they derived the spatial distribution of the galactic radio background as a

function of frequency from the postulated physical model of the galaxy. Their model contains three different sources of radio emission:

(1) A multitude of discrete radio sources widely distributed within a narrow band about the galactic equator which would result in a spatially continuous radio background, as far as the resolution of present radio telescopes is concerned

(2) Widely distributed ionized interstellar gas clouds

(3) An isotropic component of cosmic radio background, possibly of extragalactic origin

The radio galaxy derived from the above model agreed fairly well with that determined by the radio surveys available at that time, ranging from 18.3 Mc to 3 Gc (the last one over a very limited part of the celestial sphere), i.e., it agreed within the accuracy of the radio surveys. However the agreement was much better for the calculated brightness temperatures in the direction of the galactic center, the calculations being based on the same antenna beamwidths used in the original surveys at the particular frequencies. Using this model, the authors then calculated the brightness temperatures in the direction of the galactic center at the same frequencies as the radio surveys, but under the assumption of an infinitely sharp antenna beam. According to their model, the brightness temperature in the direction of the galactic center is the maximum that could be observed over the whole celestial sphere. The minimum temperature possible according to the model is that caused by the isotropic component. These values are listed in Table III and are plotted in Figure 9.

TABLE III. CALCULATED BRIGHTNESS TEMPERATURE IN THE DIRECTION OF THE GALACTIC CENTER (MAXIMUM) AND CALCULATED BRIGHTNESS TEMPERATURE OF THE ISOTROPIC COMPONENT (MINIMUM) OF THE COSMIC BACKGROUND ALONG A LINE OF SIGHT*†

Frequency (Gc)	T_b in the Direction of the Galactic Center (^oK)	T_b of Isotropic Component Along a Line of Sight (^oK)
0.0182	302,150	35,000
0.10	18,650	500
0.160	5,646	150
0.20	3,155	90
0.48	328	10
1.20	34	1
3.0	4.4	0.1

*Neglecting absorption in gas

†After Brown and Hazard [23]

According to Ko [22], the radio galaxy as it appears on more recent high-resolution surveys is incompatible with existing radio models of the galaxy which are based on relatively low-resolution surveys. Nevertheless, Figure 9 indicates that, within the accuracy of the surveys considered by Ko, the Brown and Hazard radio galaxy gives a very realistic upper bound on the brightness temperature in the direction of the galactic center and a very realistic lower bound on the brightness temperature in directions in the neighborhood of the galactic poles.

5.5.2. THE DISCRETE COSMIC RADIO-NOISE SOURCES. Kraus and Ko [8] give a list of 57 of the most intense, reliably known, cosmic radio sources. They list the position, angular size, and the flux density at the frequency or frequencies observed. They also mention all the discrete-source surveys made up to that time (1957). The various corrections to the listed position of the sources (necessary because of the earth's precession) are also given in [8]. Again, the accuracy of the measured flux densities is low, varying among observers, but is usually in the range of ±25 to ±50%.

The flux density of the discrete cosmic radio sources is also a function of frequency. The dependence on frequency can usually be represented by a spectrum index n defined by

$$S = \gamma f^n$$

where S is flux density and γ a constant. However, for many sources n varies for different parts of the radio spectrum of the source. On the basis of this definition the discrete radio sources may be divided into two classes, (1) those with a positive spectrum index, and (2) those with a negative spectrum index. The first are thermal sources and the second, nonthermal sources. Most of the discrete sources are of the nonthermal type, and though the spectrum index is not constant over the entire spectrum of the source, it is nearly constant over appreciable regions. The spectrum indices are in the range -0.5 to -1 for most discrete sources. In the microwave band, the thermal sources are more conspicuous since they are more intense at higher frequencies, although they tend to level off at very high frequencies.

Incidentally, the brightness temperature of the cosmic background may also be represented by a relation of the form

$$T_b = cf^n$$

where n varies between -2 and -2.7 over various parts of the spectrum of the cosmic background and c is a constant.

Kraus and Ko [8] show graphs of the spectrum of 11 of the most intense radio sources. Among these are Cassiopeia A and Cygnus A—the two most intense discrete sources—both of which are in the nonthermal class. Table IV lists their flux densities at a number of frequencies ranging from 81 Mc to 10 Gc.

TABLE IV. SPECTRA OF THE TWO MOST INTENSE DISCRETE COSMIC RADIO SOURCES, CASSIOPEIA A AND CYGNUS A

Discrete Source	Frequency (Gc)	Flux Density (watt-meter^{-2}-cps^{-1})
Cassiopeia A:	0.041	4×10^{-22}
	0.081	2.32×10^{-22}
	0.20	0.95×10^{-22}
	0.40	0.60×10^{-22}
	1.5	2.8×10^{-23}
	10	0.58×10^{-23}
Cygnus A:	0.041	2.3×10^{-22}
	0.081	1.42×10^{-22}
	0.20	0.9×10^{-22}
	0.40	0.43×10^{-22}
	1.5	1.5×10^{-23}
	3.0	0.72×10^{-23}

6
CONSIDERATIONS OF THE MAXIMUM AND MINIMUM EFFECTIVE ANTENNA TEMPERATURES TO BE EXPECTED

A study of the flux densities and apparent temperatures of both the solar system and cosmic discrete radio sources reveals that except for the sun their contribution to the effective antenna temperature on the earth and in aerospace is of minor importance, even for most antennas of high directivity, as compared with the contribution from the cosmic background noise and atmospheric absorption noise. However, for extremely high directivity antennas such as the 250-foot Jodrell Bank radio telescope of the University of Manachester, England, which is used to measure the flux densities and apparent temperatures of discrete sources, the contribution from the discrete sources, rather than from the cosmic background or the atmospheric emission, depending on the frequency, may dominate the effective antenna temperature. The noise data and equations presented in this report will enable one to calculate the effective antenna temperature caused by any combination of discrete and distributed sources in any particular application, both in aerospace and on the surface of the earth. It is emphasized that in any application the noise intercepted by the side lobes of the antenna from other sources than those in the main beam, especially from the earth and the sun, must be considered.

Since the contribution from the cosmic background and atmospheric emission will usually dominate the effective antenna temperature, Figure 10 has been prepared to show the composite upper and lower bounds with respect to direction on the brightness temperature of the sky as a function of frequency. Figure 10 shows that the lowest sky brightness temperatures occur between 1 and 10 Gc, with a broad minimum between 2 and 8 Gc. It is seen that even in these frequency ranges, which are exactly the ranges in which the maser amplifier shows greatest poten-

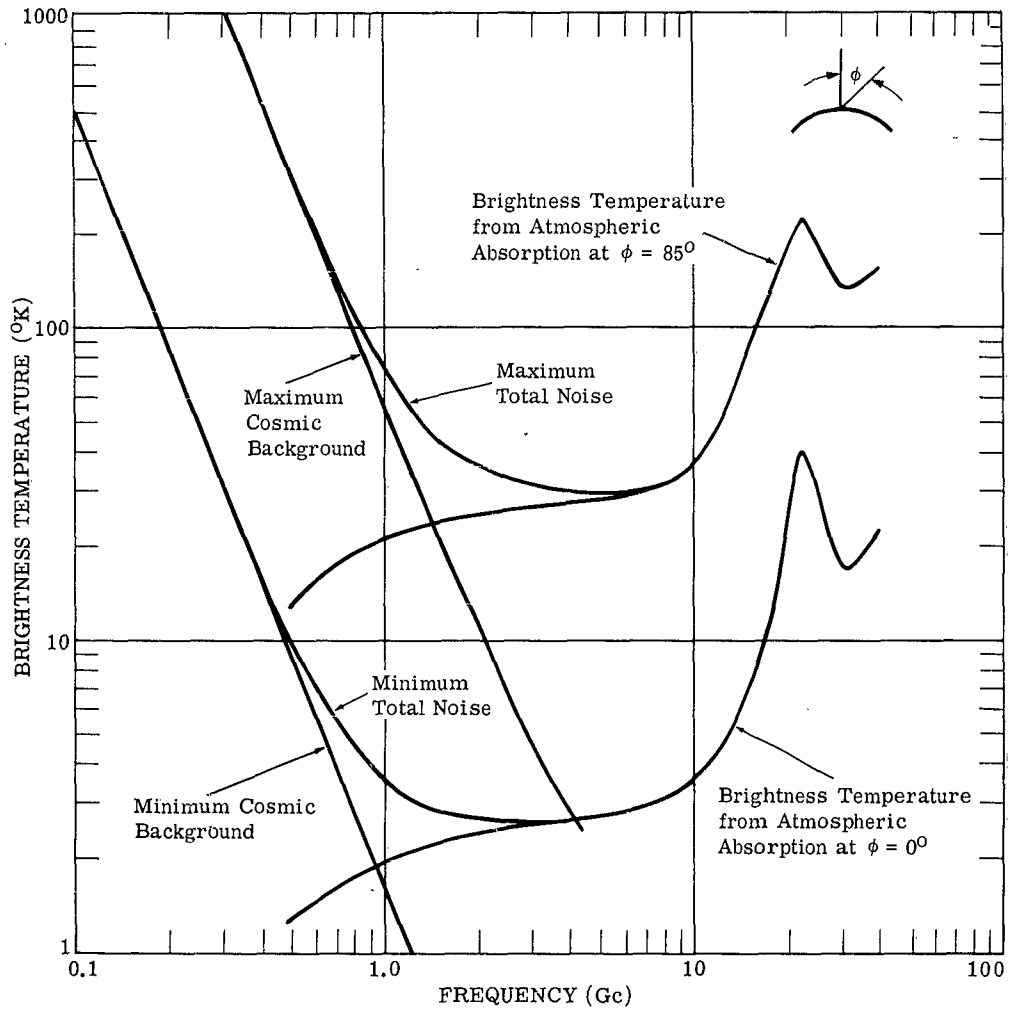

FIGURE 10. MAXIMUM AND MINIMUM BRIGHTNESS TEMPERATURE ON THE EARTH FROM A COMBINATION OF ATMOSPHERIC ABSORPTION NOISE AND COSMIC BACKGROUND NOISE

tial, the external noise will usually be either of comparable intensity or will dominate the system's internal noise temperature (see Appendix), since masers with internal noise temperatures (referred to the input terminals of the amplifier) of about $10^{o}K$ are presently available [4].

Future deep-space probes and other space missions, and the operation of interplanetary radars, may be expected to occur primarily within the plane of the ecliptic [17]. Hence it is important to consider the spatial distribution of radio noise as observed from the earth and other places within the solar system to obtain an indication of the actual noise level between the two composite noise bounds of Figure 10 that can be expected in such operations. It is known that the plane of the ecliptic passes very close to the galactic center. In addition, if one is looking at the earth from certain planets, the sun will appear within 12^{o} of the ecliptic plane. Such considerations of the range of directions in which a receiving system may be expected to operate must be employed in order to accurately determine the external noise levels in a particular situation.

If the receiving system is operating on the earth, then, because of the earth's rotation, the effective antenna temperature of a fixed antenna will be subject to diurnal and seasonal periodic variations and the periodic variation of the antenna temperature with respect to local time will advance four minutes each day, or two hours each month. For tracking antennas, the daily and seasonal antenna temperature variations are, of course, much more complex.

Appendix

EFFECTIVE INPUT NOISE TEMPERATURE OF THE OVERALL RECEIVING SYSTEM

The noise power available at the output terminals of the antenna does not, by itself, account for the total noise power available at the output of a receiving system. Noise is also generated within the internal structure of the receiver proper by various lossy passive networks and by active networks. For the purpose of analyzing the noise performance (sensitivity) of the overall receiving system, the system is conveniently divided into three sections: (1) the antenna, (2) the transmission line and other coupling devices between the antenna and the receiver, and (3) the receiver. Until now, this report has dealt exclusively with the noise available at the output terminals of the antenna. That noise power was quantitatively specified by means of the effective antenna temperature. Similarly, the noise performance of the other two sections of the receiving system can be defined in terms of temperature—called the effective input noise temperature.

The effective input noise temperature of any linear two-port transducer (passive or active) is that temperature of the input termination at which the available output noise power, from a noise-free equivalent of the transducer connected to the input termination, is equal to the available noise power from the actual transducer connected to a noise-free equivalent of the input termination. This definition applies to each pair of corresponding input and output frequencies, centered in a small frequency band Δf for which the noise powers, within Δf, at the input and output frequencies are linearly related. Thus, this definition is applicable to the heterodyne receiver for which there is, theoretically, more than one output frequency corresponding to a single input frequency and vice versa.

Again, as in the definition of the effective antenna temperature, the effective input temperature of a two-port transducer does not depend on the actual output termination. However, in contrast to the antenna, which was considered to be a single port serving as an input termination to the rest of the receiving system, the effective input temperature of a two-port transducer depends on the impedance of the input termination.

To completely describe the noise performance of a linear two-port transducer, it is necessary to specify another parameter—the attenuation or the power gain of the transducer, whichever applies to the particular transducer. The attenuation (gain) is defined as the ratio of the available signal power from the input termination of the transducer to the available output signal power from the transducer. One should note that the attenuation (gain), as defined above, depends on the input termination.

Accordingly, the noise performance of the receiver proper is completely specified by its effective input noise temperature T_r and its power gain G_r. There still remains section two of the receiving system—the transmission line and other coupling devices. This network has a physical temperature T, the temperature of the materials of which it is composed. Since this network is passive, its effective input noise temperature T_t is expressed by

$$T_t = (L - 1)\, T \tag{41}$$

where L is the attenuation of the network. This formula is obtained by a method similar to that of detailed balancing of radiation.

One can now define an effective input noise temperature T_S for the overall receiving system by combining the noise powers appearing independently in the three sections of the system. For this purpose, the antenna is replaced by an equivalent input termination to section two of the system. The impedance of this input termination is equal to the actual input impedance Z_a as seen from section two of the system. By definition of the effective antenna temperature T_a, the temperature of this input termination is equal to T_a. The effective input noise temperature T_S for the overall receiving system is defined as that temperature of the input termination at which the noise power available at the output of the system from the input termination and noise-free equivalents of sections two and three is equal to the noise power available at the output of the actual system.

The effective input noise temperature of the overall system can be calculated from the effective antenna temperature and the effective input noise temperatures of sections two and three of the receiving system. Thus, to the noise power available at the output of section two there corresponds a temperature T_2, given by

$$T_2 = \frac{T_a}{L} + \left(1 - \frac{1}{L}\right) T \tag{42}$$

and to the noise power available at the output of section three (system output) there corresponds a temperature T_3, given by

$$T_3 = \left(\frac{G_r}{L}\right) T_a + \left(1 - \frac{1}{L}\right) G_r\, T + G_r\, T_r \tag{43}$$

But from the definition of T_S, it follows that

$$T_3 = \left(\frac{G_r}{L}\right) T_S \tag{44}$$

After combining the last two equations, one obtains

$$T_S = T_a + (L - 1)\, T + L\, T_r \tag{45}$$

REFERENCES

1. W. K. Victor, R. Stevens, S. W. Golomb (Editors), Radar Exploration of Venus, Technical Report No. 32-132, Jet Propulsion Laboratory, California Institute of Technology, Pasadena, Calif., August 1, 1961.
2. J. J. Cook, M. E. Bair, L. G. Cross, The Ruby Maser: A Practical Microwave Amplifier, Report No. 2900-288-T, Institute of Science and Technology, The University of Michigan, Ann Arbor, Mich., September 1961.
3. J. J. Cook and R. W. Terhune, Radio Astronomy Masers: Test and Operational Facility, Report No. 2900-100-R, Institute of Science and Technology, The University of Michigan, Ann Arbor, Mich., May 1960.
4. R. W. DeGrasse, D. C. Hogg, E. A. Ohm, and H. E. D. Scovil, "Ultra-Low-Noise Measurements Using a Horn Reflector and a Traveling-Wave Maser," J. Appl. Phys., December 1959, Vol. 30, p. 2013.
5. J. L. Pawsey and R. N. Bracewell, Radio Astronomy, Clarendon Press, Oxford, 1955.
6. Max Planck, Theory of Heat, The Macmillan Company, New York, 1949.
7. R. A. Smith, The Physical Principles of Thermodynamics, Chapman and Hall Ltd., London, 1952.
8. J. D. Kraus and H. C. Ko, Celestial Radio Radiation, Report No. AFCRC-TN-57-557, Radio Observatory, Ohio State University, Columbus, Ohio, May 1957.
9. D. S. Heeschen, "Radio Galaxies," Scientific American, March 1962, Vol. 206, No. 3.
10. D. C. Hogg, "Effective Antenna Temperature Due to Oxygen and Water Vapor in the Atmosphere," J. Appl. Phys., September 1959, Vol. 30, No. 9.
11. D. C. Hogg and W. W. Mumford, "Effective Noise Temperature of the Sky," Microwave J., March 1960, Vol. 3, No. 3.
12. D. C. Hogg and R. A. Semplak, "The Effect of Rain and Water Vapor on Sky Noise at Centimeter Wavelengths," Bell System Tech. J., September 1961.
13. R. H. Dicke, R. Beringer, R. L. Kyhl, A. B. Vane, "Atmospheric Absorption Measurements with a Microwave Radiometer," Phys. Rev., September 1946, Vol. 70, pp. 340-348.
14. C. H. Mayer, T. P. McCullough, R. M. Sloanaker, "Measurement of Planetary Radiation at Centimeter Wavelengths," Proc. I.R.E., January 1958, Vol. 46, pp. 260-266.
15. C. H. Mayer, "Planetary Radiation at Centimeter Wavelengths," Astron. J., March 1959, Vol. 64, pp. 43-45.
16. B. F. Burke, "Noise of Planetary Origin," in D. H. Menzel (ed.), The Radio Noise Spectrum, Harvard University Press, Cambridge, Massachusetts, 1960, pp. 129-140.
17. A. G. Smith, "Extraterrestrial Noise as a Factor in Space Communications," Proc. I.R.E., April 1960, Vol. 48, pp. 593-599.

18. D. H. Menzel, "A Study on Cosmic Radio Noise Sources," in D. H. Menzel (ed.), The Radio Noise Spectrum, Harvard University Press, Cambridge, Massachusetts, 1960, pp. 151-176.

19. S. Matt and O. J. Jocomini, Microwave Radiation from the Sun, Report No. R55 ELC 8, General Electric Advanced Electronics Center, Cornell University, Ithaca, N. Y., February 18, 1955.

20. A. Maxwell, G. Swarup, A. R. Thompson, "The Radio Spectrum of Solar Activity," in D. H. Menzel (ed.), The Radio Noise Spectrum, Harvard University Press, Cambridge, Mass., 1960, pp. 101-110; also, Proc. I.R.E., January 1958, Vol. 46, pp. 142-148.

21. John E. Gibson, "Lunar Thermal Radiation at 35 KMc," Proc. I.R.E., January 1958, Vol. 46, pp. 280-286.

22. H. C. Ko, "The Distribution of Cosmic Radio Background Radiation," Proc. I.R.E., January 1958, pp. 208-215.

23. R. H. Brown and C. Hazard, "A Model of the Radio-Frequency Radiation from the Galaxy," Phil. Mag., Series 7, September 1953, Vol. 44, pp. 939-963.

24. "IRE Standards on Methods of Measuring Noise in Linear Twoports, 1959," Proc. I.R.E., Jan. 1960, Vol. 48, pp. 61-68,

DISTRIBUTION LIST

Copy No.	Addressee
1-12	Commander, Aeronautical Systems Division Wright-Patterson Air Force Base, Ohio
	(1) ATTN: ASAD
	(2) ATTN: ASAT
	(3) ATTN: ASNDCE (Harold Reece)
	(4) ATTN: ASRNGE-1
	(5-7) ATTN: ASRNGE-2 (1 repro)
	(8) ATTN: ASAPRD-RAND
	(9-11) ATTN: ASAPT
	(12) ATTN: ASAPR
13	Radio Corporation of America Defense Electronics Products Division Front and Cooper Streets Camden 2, New Jersey
	ATTN: Dr. W. C. Curtis
14	Commander, Space Systems Division AF Unit Post Office Los Angeles 45, California
	ATTN: SSTRG (Lt. Col. Lenin)
15	Commander, Air Force Systems Command Andrews Air Force Base, Washington 25, D. C.
	ATTN: RDTC
16	Deputy Chief of Staff for Research Engineering Headquarters, USAF, Washington 25, D. C.
	ATTN: Assistant for Applied Research
17	Director, Air University Library Maxwell Air Force Base, Alabama
18	Air Force Cambridge Research Laboratories Office of Aerospace Research Technical Services Division, L. G. Hanscom Field Bedford, Massachusetts
	ATTN: Research Library, Branch CRKS Stop #29
19	Commander, Rome Air Development Division Griffiss Air Force Base, New York
	ATTN: Research Library
20	Secretary, Committee on Electronics Office of Assistant Secretary of Defense Department of Defense, Washington 25, D. C.
21	Commanding Officer U. S. Army Signal Research & Development Laboratory Fort Monmouth, New Jersey
	ATTN: SIG-RA/SL - RDR
22	Office of the Chief Signal Officer Department of the Army, Washington 25, D. C.
	ATTN: Eng. and Tech. Div. SIGRD-5a
23	Chief, Bureau of Naval Weapons Department of the Navy, Washington 25, D. C.
	ATTN: Electronics Division
24	Chief, Bureau of Ships Department of the Navy, Washington 25, D. C.
	ATTN: Code 816
25	Director, U. S. Naval Research Laboratories Washington 25, D. C.
	ATTN: Code 2027
26	Bureau of Naval Weapons Fleet Readiness Representative Central, BWFRR Wright-Patterson Air Force Base, Ohio
	ATTN: Electronics Division
27	Commanding Officer U. S. Navy Electronics Laboratory San Diego 52, California
28	Commanding Officer, Office of Naval Research 346 Broadway New York 13, New York
29	Massachusetts Institute of Technology 77 Massachusetts Avenue Cambridge 39, Massachusetts
	ATTN: Mr. J. Silvey
30	Philco Corporation Research Division - Plant 37 Union Meeting & Jolly Roads Blue Bell, Pennsylvania
	ATTN: Mr. L. W. Porocopio
31-60	Armed Services Technical Information Agency Arlington Hall Station, Arlington 12, Virginia
	ATTN: TICSC

AD Div. 8/1 and 8/3

Inst. of Science and Technology, U. of Mich., Ann Arbor
EFFECTIVE ANTENNA TEMPERATURE FROM TERRESTRIAL AND COSMIC NOISE IN THE 0.1- TO 40.0-Gc BAND, by A Naparstek. Mar. 63. 40 p. incl. illus., tables, 24 refs.
(Report No. 4515-20-T)
(Contract AF 33(616)-8244) Unclassified report

This report presents a derivation of an expression for the effective antenna temperature for an antenna viewing a multitude of discrete and distributed radio-frequency noise sources. The presentation makes use of concepts, parameters, and units that have been introduced in radio astronomy for the purpose of describing measurements of radio-frequency radiation of extraterrestrial origin.

The report also presents a comprehensive review and analysis of current knowledge of and available data on radio-frequency noise of terrestrial and extraterres-

(over)

UNCLASSIFIED

I. Naparstek, A.
II. U. S. Air Force
III. Aeronautical Systems Division
IV. Contract AF 33(616)-8244

Armed Services Technical Information Agency
UNCLASSIFIED

AD Div. 8/1 and 8/3

Inst. of Science and Technology, U. of Mich., Ann Arbor
EFFECTIVE ANTENNA TEMPERATURE FROM TERRESTRIAL AND COSMIC NOISE IN THE 0.1- TO 40.0-Gc BAND, by A Naparstek. Mar. 63. 40 p. incl. illus., tables, 24 refs.
(Report No. 4515-20-T)
(Contract AF 33(616)-8244) Unclassified report

This report presents a derivation of an expression for the effective antenna temperature for an antenna viewing a multitude of discrete and distributed radio-frequency noise sources. The presentation makes use of concepts, parameters, and units that have been introduced in radio astronomy for the purpose of describing measurements of radio-frequency radiation of extraterrestrial origin.

The report also presents a comprehensive review and analysis of current knowledge of and available data on radio-frequency noise of terrestrial and extraterres-

(over)

UNCLASSIFIED

I. Naparstek, A.
II. U. S. Air Force
III. Aeronautical Systems Division
IV. Contract AF 33(616)-8244

Armed Services Technical Information Agency
UNCLASSIFIED

AD Div. 8/1 and 8/3

Inst. of Science and Technology, U. of Mich., Ann Arbor
EFFECTIVE ANTENNA TEMPERATURE FROM TERRESTRIAL AND COSMIC NOISE IN THE 0.1- TO 40.0-Gc BAND, by A Naparstek. Mar. 63. 40 p. incl. illus., tables, 24 refs.
(Report No. 4515-20-T)
(Contract AF 33(616)-8244) Unclassified report

This report presents a derivation of an expression for the effective antenna temperature for an antenna viewing a multitude of discrete and distributed radio-frequency noise sources. The presentation makes use of concepts, parameters, and units that have been introduced in radio astronomy for the purpose of describing measurements of radio-frequency radiation of extraterrestrial origin.

The report also presents a comprehensive review and analysis of current knowledge of and available data on radio-frequency noise of terrestrial and extraterres-

(over)

UNCLASSIFIED

I. Naparstek, A.
II. U. S. Air Force
III. Aeronautical Systems Division
IV. Contract AF 33(616)-8244

Armed Services Technical Information Agency
UNCLASSIFIED

AD Div. 8/1 and 8/3

Inst. of Science and Technology, U. of Mich., Ann Arbor
EFFECTIVE ANTENNA TEMPERATURE FROM TERRESTRIAL AND COSMIC NOISE IN THE 0.1- TO 40.0-Gc BAND, by A Naparstek. Mar. 63. 40 p. incl. illus., tables, 24 refs.
(Report No. 4515-20-T)
(Contract AF 33(616)-8244) Unclassified report

This report presents a derivation of an expression for the effective antenna temperature for an antenna viewing a multitude of discrete and distributed radio-frequency noise sources. The presentation makes use of concepts, parameters, and units that have been introduced in radio astronomy for the purpose of describing measurements of radio-frequency radiation of extraterrestrial origin.

The report also presents a comprehensive review and analysis of current knowledge of and available data on radio-frequency noise of terrestrial and extraterres-

(over)

UNCLASSIFIED

I. Naparstek, A.
II. U. S. Air Force
III. Aeronautical Systems Division
IV. Contract AF 33(616)-8244

Armed Services Technical Information Agency
UNCLASSIFIED